Journal of Magnetic Resonance Open 23 (2025) 100196

Contents lists available at ScienceDirect

Journal of Magnetic Resonance Open

journal homepage: www.sciencedirect.com/journal/journal-of-magnetic-resonance-open

Research article

Pushing the sensitivity boundaries of X-band EPR cryoprobe using a fast microwave switch

Uršulė Tarvydytė [a], Vidmantas Kalendra [a], Gediminas Usevičius [a], James O'Sullivan [b], Adam Brookfield [c], Alice M. Bowen [c], Jūras Banys [a], John J.L. Morton [d,e], Mantas Šimėnas [a,*]

[a] Faculty of Physics, Vilnius University, Sauletekio 3, LT-10257, Vilnius, Lithuania
[b] Amplify My Probe Ltd., London NW1 1NJ, UK
[c] The National Research Facility for Electron Paramagnetic Resonance, Department of Chemistry and Photon Science Institute, The University of Manchester, Oxford Road, Manchester M13 9PL, UK
[d] London Centre for Nanotechnology, University College London, London WC1H 0AH, UK
[e] Department of Electronic & Electrical Engineering, University College London, London WC1E 7JE, UK

ARTICLE INFO

Dataset link: http://dx.doi.org/10.18279/MIDAS.SPECTR.203438

Keywords:
Pulsed EPR
Cryoprobe
LNA
Sensitivity
Noise

ABSTRACT

We present a new design of an X-band EPR cryoprobe based on a fast microwave switch and a cryogenic low-noise microwave amplifier that are placed close to the sample in the same cryostat. The probehead supports high-power (100 W) pulsed EPR experiments and is compatible with standard EPR resonators and samples. In contrast to the directional coupler design of the EPR cryoprobe reported previously, the fast microwave switch fully isolates the microwave amplifier from input thermal noise without microwave power suppression allowing us to approach the sensitivity limit of cryoprobes for pulsed EPR experiments. We benchmark the performance of our cryoprobe setup against a standard commercial EPR instrument revealing a significant sensitivity improvement, which reduces the measurement time by a factor of about 250× at 6 K sample temperature. We also show that the sensitivity of our new X-band cryoprobe design matches that of a standard Q-band setup for double electron–electron resonance experiments.

1. Introduction

Inspired by the success of NMR cryoprobes [1–4] and previous efforts toward EPR cryoprobes [5–8], we have recently reported a boost in X- and Q-band EPR sensitivity using EPR cryoprobes containing cryogenic microwave low noise amplifiers (LNAs) [9,10]. In our setups, the LNA and its protection circuit were placed close to the sample in the same cryostat, while maintaining compatibility with commercial spectrometers and typical samples. For high-power pulsed EPR experiments, the X-band EPR cryoprobe provided a significant sensitivity improvement compared to a commercial spectrometer exceeding a factor of 7× in voltage signal-to-noise ratio (SNR) at temperatures below 10 K, which gradually diminished to about 2× at room temperature [9]. The sensitivity improvement offered by the more complex Q-band EPR cryoprobe was about 6× below 10 K [10]. The sensitivity enhancement provided by the cryoprobes has already enabled important EPR studies of some intricate spin systems that would otherwise be nearly impossible [11–13].

The obtained sensitivity gain in the aforementioned EPR cryoprobe designs mostly originates from three factors. First of all, thermal microwave noise generated by the microwave components is substantially lower, as they are cooled down together with the sample, while the employed cryogenic LNAs have better noise characteristics than ordinary LNAs. Secondly, the microwave circuits dedicated to guide microwaves and protect the LNA proved to be less lossy compared to the commercial spectrometers, partly due to the significantly shorter microwave path between the resonator and the LNA. Lastly, the cryoprobes also suppress input thermal noise, which propagates from outside of the cryostat down to the LNA via the input microwave path. A suppression of input thermal noise is necessary to achieve a significant sensitivity improvement, as evident from our recent study of an external EPR cryoprobe, where minimal suppression was realized and thus only moderate sensitivity gains were observed [14]. A partial suppression of the input thermal noise in our previous X- and Q-band cryoprobe designs was enabled by directional couplers, which were also used to guide the microwave signals to and from the resonator (see Fig. 1a) [9,10]. The directional coupler approach was also recently implemented in a W-band cryoprobe by Blank's group [15]. However, in addition to input thermal noise, the directional coupler also significantly reduces the power of microwave excitation. For example, a full suppression of input

* Corresponding author.
E-mail address: mantas.simenas@ff.vu.lt (M. Šimėnas).

https://doi.org/10.1016/j.jmro.2025.100196
Received 7 December 2024; Received in revised form 11 March 2025; Accepted 18 March 2025
Available online 3 April 2025

Journal of Magnetic Resonance Open 23 (2025) 100196

thermal noise would be achieved using a 20 dB coupler, which would increase the duration of the π-pulse by a factor of 10. For standard EPR cavities, such a highly limited excitation bandwidth would eliminate the sensitivity gain provided by the cryoprobe. Thus, an alternative microwave circuit that could simultaneously fully suppress input thermal noise, minimally reduce excitation power and protect the LNA is highly desirable, as it would allow to approach the sensitivity limit of EPR cryoprobes.

A single-pole double-throw (SPDT) microwave switch, with the common port connected to a microwave resonator, satisfies these requirements for pulsed EPR experiments (see Fig. 1), as has been demonstrated in specialized cryostats in the field of quantum technologies [16]. In such a configuration, the switch is switched to the input path, when high-power microwave pulses are expected (Fig. 1b). After the spin system is excited, the switch is switched to the cryogenic LNA path resulting in the echo amplification (Fig. 1c,d). Simultaneously, the LNA is isolated from the input path resulting in suppression of the input thermal noise. However, for such a cryoprobe design to be compatible with the state-of-the-art EPR experiments, the switch must satisfy several technical requirements that are difficult to meet in practise. First of all, the switch must function at cryogenic temperatures, which poses a significant challenge for some semiconductor platforms. In addition, it must be sufficiently fast (switching time of tens of ns) to avoid prolongation of the undesirable spectrometer deadtime. The switch must also handle high microwave power to enable high-bandwidth excitation of the spin system. Lastly, it should have low microwave loss and high isolation essential to ensure a sufficient protection of the LNA and suppression of the input thermal noise.

Here, we report design, construction and benchmarking of an X-band EPR cryoprobe based on a fast SPDT microwave switch, a cryogenic LNA and a commercial split ring resonator. In addition to standard sample access and resonator coupling capabilities, the cryoprobe provides a full suppression of the input thermal noise, while permitting excitation pulse powers up to 100 W. We demonstrate the performance of our setup by performing pulsed EPR experiments including double electron–electron resonance (DEER) of ordinary samples. Our new design approaches the sensitivity limit of EPR cryoprobes providing a highly significant voltage SNR improvement of 16× at 6 K, which gradually approaches 2.5× at room temperature.

2. Probehead design

Our cryoprobe is based on a Qorvo TGS2352-2-SM SPDT fast microwave switch, which is sufficiently fast (< 35 ns switching time) and operates at temperatures even below 10 K, while maintaining low loss and sufficiently high isolation (see Figure S1). The switch is controlled using a signal from the "Receiver Protection 2" channel in the Bruker console, converted to the required control logic (0 V/−40 V) using a home-built logic board based on a Monzite MDI2354Q switch driver. The specified continuous-wave microwave power for this switch is 20 W, while the peak power is about 100 W, as determined by our pulsed EPR experiments using a pulse of 40 ns duration and a shot repetition time of 1 ms. Around this power level, we observed that the switch starts to operate in the compression mode, while at even higher power levels it exhibits signs of degradation. Note that we did not observe any switch degradation effects at 100 W power. To achieve sufficiently short π-pulse durations (32 ns or shorter) at such limited power levels, we used a Bruker MS-3 split ring X-band microwave resonator, which has a high conversion factor and is compatible with 3 mm outer-diameter EPR tubes.

The microwave circuit of our cryoprobe is presented in Fig. 2, and its working principle is based on the design illustrated in Fig. 1. At the heart of the cryoprobe there is a cryogenic LNC4_16B LNA from Low Noise Factory (36 dB gain, 4 K noise temperature at 4 K and 9.5 GHz). For additional protection of the LNA from microwave power leakage through the switch, we used a Narda-MITEQ LIM301 limiter (500 W

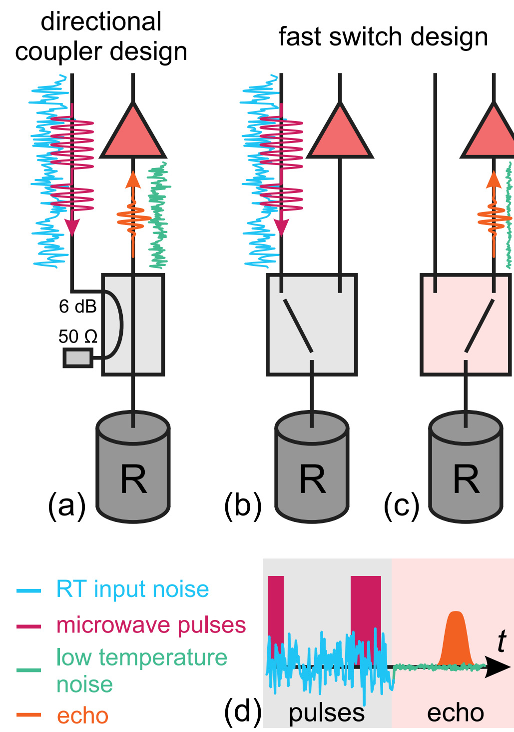

Fig. 1. Schematic representations of the low-temperature operation of the EPR cryoprobes based on (a) a 6 dB directional coupler and (b,c) a fast SPDT microwave switch. (b,d) The switch is switched to the input path (room temperature thermal noise), when high power microwave pulses are expected. (c,d) After the last pulse, the switch is switched to the cryogenic LNA path ensuring echo amplification and low temperature noise. A switch with strong isolation offers significantly greater suppression of input thermal noise compared to a 6 dB directional coupler.

peak power, 130 mW flat leakage, < 200 ns recovery time, 0.1% duty cycle, ∼ 1 dB insertion loss). Our cryoprobe fits inside typical EPR cryostats (Oxford CF935, and Cryogenic EPR system), while retaining conventional sample access and resonator coupling capabilities. The LNA is thermalized to the temperature of the sample via a C110 copper bracket extending below the resonator to the bottom of the cryostat. A photograph of our probehead is given in Figure S2.

We note that the cryoprobe operates in a quasi transmission mode, as it has input and output microwave ports that must be connected to the EPR bridge, while typical EPR spectrometers are designed to operate only in reflection and thus have only one port. As in our previous works [9,10,14], we address this problem through a simple modification of the microwave bridge in which we bypass the internal circulator.

3. Experimental and calculation details

3.1. Benchmark of sensitivity improvement

To benchmark the sensitivity improvement provided by our setup, we performed pulsed EPR experiments using a Bruker ELEXSYS E580 spectrometer equipped with a 1 kW traveling-wave tube (TWT) amplifier. For these experiments, we placed a small amount of the Bruker DEER test sample (E3005315) in a 3 mm outer diameter EPR tube. The SNR improvement was characterized using a Hahn echo pulse sequence ($\pi/2$-τ-π-τ-echo) with two-step phase cycling. A typical π-pulse duration in our experiments was 32 ns, which was readily achieved using the overcoupled Bruker MS-3 resonator (Q-factor ∼ 100, conversion factor ∼ 2 G/$\sqrt{\text{W}}$).

To avoid saturation of the digitizer, the interpulse delay τ was adjusted to produce a sufficiently weak echo signal. Depending on

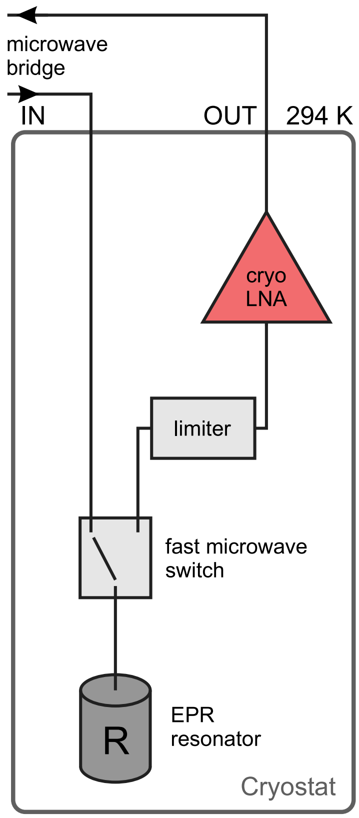

Fig. 2. Schematic of the microwave circuit within our X-band EPR cryoprobe based on a fast microwave switch. The probehead is connected to the microwave bridge using two microwave ports. In practice, all microwave components are closely packed close to the resonator.

the sample temperature, the shot repetition time was chosen to be sufficiently long to allow full recovery of the signal.

The SNR and its uncertainty were determined using 10 separate measurements of the Hahn echo. The traces were corrected by subtracting constant backgrounds, which proved to be almost negligible. The intensity of the spin signal was taken as a maximum of the echo obtained by fitting a Gaussian peak function, while noise was calculated as the standard deviation of the signal far away from the echo (at least 500 data points were used for noise calculation).

The SNR improvement provided by our cryoprobe was benchmarked against the standard reflection probehead. The resonator coupling arm was tightly fixed to avoid potential variations during switching between both setups. All parameters, except for the microwave power and tiny changes in the microwave frequency and magnetic field, were kept constant in both measurements. The microwave power was adjusted to yield the same duration of the π-pulse in both cases, and the field position was verified by the echo-detected field sweep (EDFS) experiments obtained using the same Hahn echo pulse sequence.

3.2. DEER experiments

We also compared the DEER sensitivity of our X-band cryoprobe with that of a standard Q-band setup. The DEER experiments of the Bruker DEER sample were performed at 50 K using the four-pulse DEER sequence ($\pi/2$-τ_1-π-t_1-π_{pump}-($\tau_1+\tau_2-t_1$)-π-τ_2-echo) [17]. Measurements at X-band were performed using the cryoprobe with the overcoupled Bruker MS-3 resonator, while Q-band experiments were carried out using a 3 mm dual mode resonator (QT-IIW) and a Bruker ELEXSYS 580 FT spectrometer equipped with a 300 W TWT. The DEER traces were acquired using $\tau_1 = 130$ ns, $\tau_2 = 5$ µgreeks, and the initial value of $t_1 = 80$ ns.

For X-band experiments, the microwave power was optimized to yield 32 ns duration for all pump and observer pulses. The traces were collected using 55 MHz frequency difference between the observer and pump pulses, and seven-step nuclear modulation averaging with an averaging time step of 10 ns. For Q-band measurements, the duration of all observer pulses was set 32 ns, while the pump pulse was 28 ns. No nuclear modulation averaging was applied. The frequency separation between the observer and pump pulses was 60 MHz. In both cases, a two-step phase cycling, an 8 ns increment of the time-domain traces, and 3 ms shot repetition time were used.

The data analysis was performed using user-independent data processing with the ComparativeDEERAnalyzer version 2.0 with DEERNet Spinach SVN Rev 5662 [18] and DeerLab 0.9.1 [19].

3.3. Calculation of sensitivity improvement

The SNR improvement factor was calculated using the approach developed in our previous works [10,14], which is based on the effective noise temperature formalism [5]. We define the sensitivity improvement provided by the cryoprobe as the output voltage SNR ratio between the cryoprobe (C) and unmodified (U) setups:

$$\frac{\mathrm{SNR}_{\mathrm{out}}^{\mathrm{C}}}{\mathrm{SNR}_{\mathrm{out}}^{\mathrm{U}}} = \sqrt{\frac{F^{\mathrm{U}}}{F^{\mathrm{C}}}\frac{T_{\mathrm{in}}^{\mathrm{U}}}{T_{\mathrm{in}}^{\mathrm{C}}}}. \tag{1}$$

Here, F and T_{in} denote the noise factor of the microwave circuit and the noise temperature at its input, respectively. The noise factor can be calculated from the total effective noise temperature T_{e} as

$$F = 1 + \frac{T_{\mathrm{e}}}{T_{\mathrm{in}}}, \tag{2}$$

where T_{e} can be obtained using the Friis equation [10,14,20].

In our calculations, we assume $T_{\mathrm{in}}^{\mathrm{U}} = 294$ K, independent of the sample temperature, since, in a standard setup, the resonator is not isolated from room temperature thermal noise. In contrast, a fast microwave switch used on our cryoprobe has a sufficiently high isolation (see Figure S1) providing a full suppression of the input thermal noise at temperatures typically used in EPR spectroscopy. Thus, we set $T_{\mathrm{in}}^{\mathrm{C}} = T_S$, where T_S is sample temperature.

To calculate the noise factors, we measured microwave losses of our setup using a Copper Mountain S5243 vector network analyzer (VNA). The gain and noise temperature of the cryogenic LNA was taken from the manufacturer specifications, while, as in our previous work, the noise temperature of the bridge amplifier was assumed to be 250 K [14].

4. Results and discussion

The performance of our new cryoprobe was investigated by measuring the Hahn echo of the Bruker DEER sample and comparing it to the unmodified setup. A comparison of the echoes obtained at 6 K are presented in Fig. 3a revealing that our cryoprobe provides a significant voltage SNR improvement by a factor of about 16×, which translates to a measurement time reduction by a factor of 250× at this temperature.

To study the temperature dependence of the SNR improvement, we performed Hahn echo experiments at different sample temperatures ranging from 6 K up to room temperature (see Fig. 4). Since the cryoprobe warms up with the sample, the sensitivity improvement gradually decreases reaching a value of about 2.4× at room temperature (Fig. 3b). As also observed for our previous cryoprobe designs [9,10,14], the remaining improvement originates from less lossy microwave circuit and lower noise temperature of the LNA compared to the Bruker setup.

We measured the microwave losses of our cryoprobe and unmodified setups using a VNA (Figure S3) allowing us to compare the experimentally obtained temperature dependence of the sensitivity improvement with the theoretical model given by Eq. (1). Provided a full suppression of the input thermal noise ($T_{in}^{C} = T_S$), our calculations show a good agreement with the experimental results (Fig. 4) indicating the validity of our assumptions regarding the origin of the sensitivity improvement. A small discrepancy may originate from the unaccounted sources of uncertainty, which are difficult to quantify in practise (e.g. temperature gradients, changes of microwave loss with temperature).

Our model also allows us to predict the sensitivity limit for almost ideal EPR cryoprobe having a lossless LNA protection circuit, where the noise factor is determined solely by the noise temperature of the currently employed LNA. At 6 K, such a cryoprobe would provide the SNR improvement factor of 20.8× showing that our current cryoprobe design is close to the theoretical sensitivity limit.

Note that despite microwave power limitation imposed by the fast microwave switch (see Probehead design), the Hahn echo experiments were performed using a π-pulse of 32 ns duration, which was facilitated by the high conversion factor Bruker MS-3 resonator. At the maximum appropriate power level, we managed to obtain an even shorter π-pulse duration approaching 20 ns. These results demonstrate that our new design can reach significant sensitivity improvement of pulsed EPR experiments, while sustaining high-bandwidth excitation. For comparison, the shortest π-pulse duration using a lower conversion factor Bruker MD-5 resonator was about 40 ns.

For comparison, we also performed measurements and calculations of the sensitivity improvement provided by the cryoprobe based on a 6 dB directional coupler and the Bruker MD-5 resonator. The results are also presented in Fig. 4 revealing that the SNR enhancement factor ranges from 1.2× at room temperature to 6.5× at 10 K in a good agreement with our previous study [9]. These findings demonstrate that the new cryoprobe based on a fast microwave switch significantly outperforms the 6 dB directional coupler design by a factor of about 2×.

For a fairer comparison between the directional coupler and switch cryoprobe setups, we also calculated the sensitivity improvement expected for a cryoprobe based on a 10 dB directional coupler (see Fig. 4). In this case, the maximum microwave power is the same as for the switch design (100 W), while the suppression of input thermal noise is slightly greater ($T_{in}^{C} \geq 30$ K) compared to the 6 dB coupler case ($T_{in}^{C} \geq 75$ K). Our calculations show that in this case the switch cryoprobe still outperforms the 10 dB coupler design by a significant factor of about 1.5×.

We also compared the sensitivity of our switch cryoprobe design with a standard commercial Q-band TWT setup for DEER experiments at 50 K. In both cases, the same Bruker DEER sample (3 mm outer diameter EPR tube) fully filling both resonators, identical measurement times, and optimized conditions for each setup were used. The measured primary DEER data are presented in Figure S5, while the corresponding background-corrected form factors are shown in Fig. 5a revealing similar traces. In both cases, the corresponding distance distributions (Fig. 5b) exhibit a clear peak at 2 nm, where a slightly greater broadening is observed for the X-band cryoprobe data. The SNR comparison, based on the modulation depths and fit residuals of the time-domain data (inset in Fig. 5a), yielded a voltage SNR ratio of about 1.2 slightly favoring the Q-band setup. Note that the more sensitive state-of-the-art home-built Q-band setup would provide a slightly greater sensitivity difference [21]. Overall, our measurements demonstrate that the performance of our X-band cryoprobe for DEER experiments at 50 K becomes comparable to that of the significantly more expensive Q-band setups.

The limited microwave power of the cryoprobe setup prevented us from using shorter than 32 ns pump pulses for the DEER experiments. Our theoretical predictions of the DEER sensitivity indicate that using the 12 ns pump pulse achievable with the unmodified X-band probeheads [21] would provide about 1.6× higher DEER sensitivity compared to the 32 ns pump pulse. This effectively reduces the DEER SNR improvement provided by our cryoprobe to about 5.6× instead of 9× at 50 K. By taking the bandwidth limitations into account, the state-of-the-art home-built Q-band setup [21] would outperform our X-band cryoprobe by a factor of about 3×.

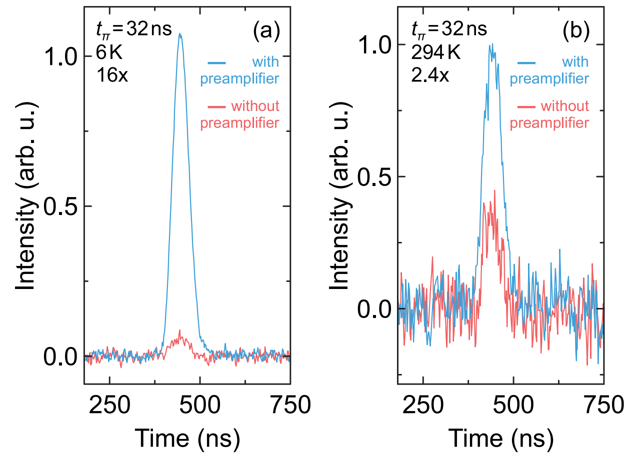

Fig. 3. Hahn echoes of the Bruker DEER sample obtained at (a) 6 K and (b) room temperature with and without the cryoprobe with the corresponding voltage SNR improvements of (a) 16× and (b) 2.4×. The echoes are normalized to the noise level. Experimental parameters: (a) τ = 5 μgreeks, 4 averages, t_π = 32 ns, and (b) τ = 0.5 μgreeks, 10 averages, t_π = 32 ns.

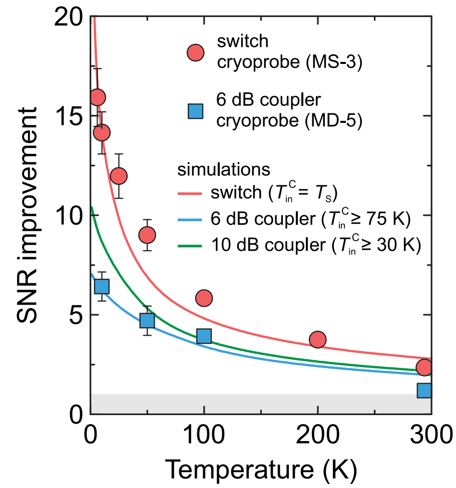

Fig. 4. SNR improvement vs. sample (cryoprobe) temperature measured using Hahn echo experiments for the switch and 6 dB coupler cryoprobes. The solid curves show the calculated SNR improvements for the switch ($T_{in}^{C} = T_S$), 6 dB coupler ($T_{in}^{C} \geq 75$ K) and 10 dB coupler ($T_{in}^{C} \geq 30$ K) cryoprobes based on the microwave losses of the cryoprobe and Bruker setups. The gray region marks SNR improvement less than one. If not indicated, the error bar is smaller than the size of the data point. (For interpretation of the references to color in this figure legend, the reader is referred to the web version of this article.)

Further improvements of the new cryoprobe design are possible and are directly related to the properties of the fast microwave switch. A switch having a better isolation would allow removal of the limiter from the LNA protection circuit further boosting the sensitivity improvement by about 10% provided the microwave losses of the switch remain the same. In addition, a switch capable of higher power handling is also desirable, as it would enable pulsed EPR experiments with high-bandwidth pulses using dielectric ring and other resonators that have relatively low conversion factors.

5. Conclusions

In this work, we constructed and tested a new design of X-band EPR cryoprobe based on a fast SPDT microwave switch and a cryogenic

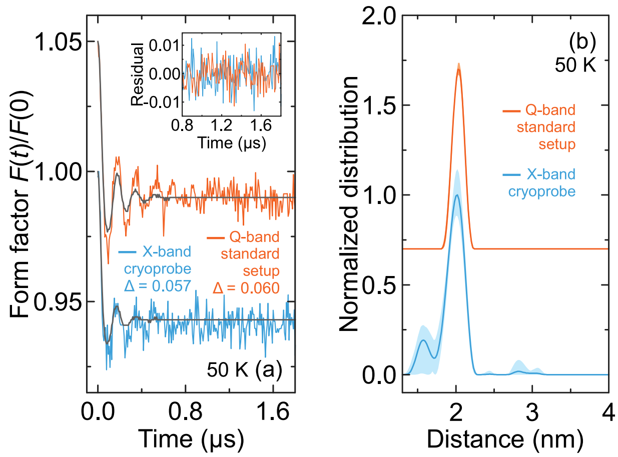

Fig. 5. (a) Normalized DEER time-domain traces of the Bruker DEER sample obtained at 50 K using the X-band EPR cryoprobe and the Q-band setups. The Q-band trace is shifted by 0.05. (b) The corresponding distance distributions obtained by Tikhonov regularization. The gray curves in (a) are fits to the time-domain data. The obtained modulation depths Δ are indicated in the legend. Inset shows the time-domain residual, which is used to compare the sensitivity between both setups. The shaded regions in (b) mark the uncertainty estimate of the distance distributions. (For interpretation of the references to color in this figure legend, the reader is referred to the web version of this article.)

low-noise microwave preamplifier. The new cryoprobe is compatible with commercial microwave resonators and conventional samples. In contrast to cryoprobes based on directional coupler, the new design fully suppresses input thermal noise while maintaining high-power up to 100 W pulse excitation. This allows us to approach the sensitivity limit of EPR cryoprobes using short π-pulse durations.

Measurements of the Hahn echo experiments demonstrated a highly significant SNR improvement by a factor of 16× at 6 K, which gradually decayed to about 2.5× at room temperature. As discussed in our previous works, the observed decrease in sensitivity enhancement with increasing sample temperature could be partially eliminated by separately cooling the LNA and the sample. We also demonstrated that the enhanced sensitivity of our new X-band cryoprobe closely rivals that of the considerably more expensive Q-band TWT setups for DEER experiments conducted at 50 K.

In principle, the presented cryoprobe design is also compatible with other frequency bands provided that suitable switches are available. Note that the previously reported Q-band cryoprobe based on a 10 dB directional coupler prevented us from reaching state-of-the-art pulse durations with a 10 W solid-state amplifier [10]. This limitation can be resolved using the fast switch design. The switch approach is also fully compatible with EPR microresonators, where significantly lower powers are used eliminating the need for high-power handling capabilities of the switch.

In general, the obtained sensitivity gains can be used to reduce both spin concentration and sample volumes, thereby enabling advanced X-band EPR experiments (such as hyperfine [22] and dipolar [17,23–25] spectroscopies) with significantly improved sensitivity.

CRediT authorship contribution statement

Uršulė Tarvydytė: Writing – review & editing, Investigation. **Vidmantas Kalendra:** Writing – review & editing, Resources, Methodology, Investigation. **Gediminas Usevičius:** Writing – review & editing, Investigation. **James O'Sullivan:** Writing – review & editing, Methodology, Conceptualization. **Adam Brookfield:** Writing – review & editing, Resources, Investigation. **Alice M. Bowen:** Writing – review & editing, Resources, Investigation, Funding acquisition. **Jūras Banys:** Writing – review & editing, Resources, Project administration, Funding acquisition. **John J.L. Morton:** Writing – review & editing, Validation, Resources, Methodology, Conceptualization. **Mantas Šimėnas:** Writing – review & editing, Writing – original draft, Visualization, Validation, Supervision, Software, Resources, Project administration, Methodology, Investigation, Funding acquisition, Formal analysis, Data curation, Conceptualization.

Declaration of competing interest

The authors declare the following financial interests/personal relationships which may be considered as potential competing interests: Mantas Simenas reports a relationship with Amplify My Probe Ltd. that includes: equity or stocks. James O'Sullivan reports a relationship with Amplify My Probe Ltd. that includes: equity or stocks. Vidmantas Kalendra reports a relationship with Amplify My Probe Ltd. that includes: equity or stocks.

Acknowledgments

The research reported in this publication was supported by funding from the European Union HORIZON-MSCA-2021-PF-01 Marie Skłodowska-Curie Fellowship (Project ID: 101064200; SPECTR, https://epr.ff.vu.lt/spectr) (M.Š., J.B.), and European Research Council (ERC) under the European Union's Horizon 2020 research and innovation programme (Grant agreement No. 771493) (J.J.L.M.). This work has also received funding from the Engineering and Physical Sciences Research Council (EP/W005794/1) (J.J.L.M.), and the Research Council of Lithuania (LMTLT), agreement No. S-LLT-23-1 (V.K., G.U.). A.M.B. and A.B. are grateful to the Engineering and Physical Sciences Research Council for support of the National Research Facility for EPR (EP/W014521/1, EP/X034623/1, EP/Z530670/1, OPP651-UKRI388, NS/A000055/1, EP/V035231/1, and EP/S033181/1). A.M.B. is grateful to The Royal Society and the EPSRC for a Dorothy Hodgkin Fellowship (DH160004 and DHF R 221018), the University of Manchester for a Dame Kathleen Ollerenshaw Fellowship, and the Royal Society of Chemistry for a Community for Analytical and Measurement Science fellowship (CAMS Fellowship 2020 ACTF ref 600310/09). The authors thank Prof. Gunnar Jeschke for the assistance in the theoretical estimation of DEER sensitivity.

Appendix A. Supplementary data

Supplementary material related to this article can be found online at https://doi.org/10.1016/j.jmro.2025.100196.

Data availability

Data needed to evaluate the conclusions in the paper can be found at http://dx.doi.org/10.18279/MIDAS.SPECTR.203438. Additional data related to this paper may be requested from the authors.

References

[1] P. Styles, N. Soffe, C. Scott, D. Crag, F. Row, D. White, P. White, A high-resolution NMR probe in which the coil and preamplifier are cooled with liquid helium, J. Magn. Reson. (1969) 60 (1984) 397–404.
[2] P. Styles, N.F. Soffe, C.A. Scott, An improved cryogenically cooled probe for high-resolution NMR, J. Magn. Reson. (1969) 84 (1989) 376–378.
[3] L. Darrasse, J.-C. Ginefri, Perspectives with cryogenic RF probes in biomedical MRI, Biochimie 85 (2003) 915–937.
[4] H. Kovacs, D. Moskau, M. Spraul, Cryogenically cooled probes - a leap in NMR technology, Prog. Nucl. Magn. Reson. Spectrosc. 46 (2005) 131–155.
[5] S. Pfenninger, W. Froncisz, J. Hyde, Noise analysis of EPR spectrometers with cryogenic microwave preamplifiers, J. Magn. Reson. Ser. A 113 (1995) 32–39.
[6] G.A. Rinard, R.W. Quine, R. Song, G.R. Eaton, S.S. Eaton, Absolute EPR spin echo and noise intensities, J. Magn. Reson. 140 (1999) 69–83.
[7] R. Narkowicz, H. Ogata, E. Reijerse, D. Suter, A cryogenic receiver for EPR, J. Magn. Reson. 237 (2013) 79–84.

[8] Y. Artzi, Y. Twig, A. Blank, Induction-detection electron spin resonance with spin sensitivity of a few tens of spins, Appl. Phys. Lett. 106 (2015) 084104.

[9] M. Šimėnas, J. O'Sullivan, C.W. Zollitsch, O. Kennedy, M. Seif-Eddine, I. Ritsch, M. Hülsmann, M. Qi, A. Godt, M.M. Roessler, G. Jeschke, J.J. Morton, A sensitivity leap for X-band EPR using a probehead with a cryogenic preamplifier, J. Magn. Reson. 322 (2021) 106876.

[10] V. Kalendra, J. Turčak, G. Usevičius, H. Karas, M. Hülsmann, A. Godt, G. Jeschke, J. Banys, J.J. Morton, M. Šimėnas, Q-band EPR cryoprobe, J. Magn. Reson. 356 (2023) 107573.

[11] K.H. Richardson, J.J. Wright, M. Šimėnas, J. Thiemann, A.M. Esteves, G. McGuire, W.K. Myers, J.J.L. Morton, M. Hippler, M.M. Nowaczyk, G.T. Hanke, M.M. Roessler, Functional basis of electron transport within photosynthetic complex i, Nat. Commun. 12 (2021) 5387.

[12] J. O'Sullivan, O.W. Kennedy, C.W. Zollitsch, M. Šimėnas, C.N. Thomas, L.V. Abdurakhimov, S. Withington, J.J. Morton, Spin-resonance linewidths of bismuth donors in silicon coupled to planar microresonators, Phys. Rev. Appl. 14 (2020) 064050.

[13] M. Šimėnas, J. O'Sullivan, O.W. Kennedy, S. Lin, S. Fearn, C.W. Zollitsch, G. Dold, T. Schmitt, P. Schüffelgen, R.-B. Liu, J.J.L. Morton, Near-surface $^{125}Te^{+}$ spins with millisecond coherence lifetime, Phys. Rev. Lett. 129 (2022) 117701.

[14] V. Kalendra, J. Turčak, J. Banys, J.J. Morton, M. Šimėnas, X- and Q-band EPR with cryogenic amplifiers independent of sample temperature, J. Magn. Reson. 346 (2023) 107356.

[15] M. Jbara, O. Zgadzai, W. Harneit, A. Blank, Cryogenic W-band electron spin resonance probehead with an integral cryogenic low noise amplifier, Appl. Magn. Reson. (2024).

[16] R.M. Jock, Spin Dynamics of Electrons Confined in Silicon Heterostructures (Ph.D. thesis), Princeton University, 2015.

[17] M. Pannier, S. Veit, A. Godt, G. Jeschke, H. Spiess, Dead-time free measurement of dipole-dipole interactions between electron spins, J. Magn. Reson. 142 (2000) 331–340.

[18] S.G. Worswick, J.A. Spencer, G. Jeschke, I. Kuprov, Deep neural network processing of DEER data, Sci. Adv. 4 (2018) eaat5218.

[19] L. Fábregas Ibáñez, G. Jeschke, S. Stoll, DeerLab: a comprehensive software package for analyzing dipolar electron paramagnetic resonance spectroscopy data, Magn. Reson. 1 (2020) 209–224.

[20] H. Friis, Noise figures of radio receivers, Proc. IRE 32 (1944) 419–422.

[21] Y. Polyhach, E. Bordignon, R. Tschaggelar, S. Gandra, A. Godt, G. Jeschke, High sensitivity and versatility of the DEER experiment on nitroxide radical pairs at Q-band frequencies, Phys. Chem. Chem. Phys. 14 (2012) 10762–10773.

[22] Y. Deligiannakis, M. Louloudi, N. Hadjiliadis, Electron spin echo envelope modulation (ESEEM) spectroscopy as a tool to investigate the coordination environment of metal centers, Coord. Chem. Rev. 204 (2000) 1–112.

[23] G. Jeschke, M. Pannier, A. Godt, H. Spiess, Dipolar spectroscopy and spin alignment in electron paramagnetic resonance, Chem. Phys. Lett. 331 (2000) 243–252.

[24] P.P. Borbat, J.H. Freed, Multiple-quantum ESR and distance measurements, Chem. Phys. Lett. 313 (1999) 145–154.

[25] S. Milikisyants, F. Scarpelli, M.G. Finiguerra, M. Ubbink, M. Huber, A pulsed EPR method to determine distances between paramagnetic centers with strong spectral anisotropy and radicals: The dead-time free RIDME sequence, J. Magn. Reson. 201 (2009) 48–56.